The impact of solar spectral irradiance variability on middle atmospheric ozone

Aimee W. Merkel,[1] Jerald W. Harder,[1] Daniel R. Marsh,[2] Anne K. Smith,[2] Juan M. Fontenla,[1] and Thomas N. Woods[1]

Received 24 March 2011; revised 15 May 2011; accepted 18 May 2011; published 2 July 2011.

[1] This study presents the impact of solar spectral irradiance (SSI) variability on middle atmospheric ozone over the declining phase of solar cycle 23. Two different types of spectral forcing are applied to the Whole Atmosphere Community Climate Model (WACCM) to simulate the ozone response between periods of quiet and high solar activity. One scenario uses the solar proxy reconstructions model from the Naval Research Laboratory (NRLSSI), and the other is based on SSI observations from the Solar Radiation and Climate Experiment (SORCE). The SORCE observations show 3–5 times more variability in ultraviolet (UV) radiation than predicted by the proxy model. The NRLSSI forcing had minimal impact on ozone, however, the higher UV variability from SORCE induced a 4% reduction in ozone concentration above 40 km at solar active conditions. The model result is supported by 8 years (2002–2010) of ozone observations from the Sounding of the Atmosphere using Broadband Emission Radiometry (SABER) instrument. The SABER ozone variations have greater similarity with the SORCE SSI model simulations. The model and satellite data suggests that the ozone response is due to enhanced photochemical activity associated with larger UV variability. **Citation:** Merkel, A. W., J. W. Harder, D. R. Marsh, A. K. Smith, J. M. Fontenla, and T. N. Woods (2011), The impact of solar spectral irradiance variability on middle atmospheric ozone, *Geophys. Res. Lett.*, *38*, L13802, doi:10.1029/2011GL047561.

1. Introduction

[2] The SSI is an important factor in establishing the Earth's atmospheric composition and structure. The combined solar spectral irradiance observations from the Solar Stellar Irradiance Comparison Experiment (SOLSTICE) and the Spectral Irradiance Monitor (SIM) on the SORCE satellite provide trends of the UV, visible and near-IR variability simultaneously. Although the time series of the SORCE data does not cover a full solar cycle, the measurements indicate a factor of 3–5 larger UV variability between year 2004 (solar active) and year 2007 (solar quiet) than that of semi-empirical models of SSI [*Harder et al.*, 2009]. The SIM irradiance measurements have an accuracy of better than 2% [*Harder et al.*, 2010]. Based on the comparison of the two independent SIM channels, long-term uncertainty in the 200–300 nm region is ~0.5–0.1%, from 310–400 nm it is ~0.2–0.05%, and in the 400–1600 nm range it is better than 0.05%. Currently there is no direct validation through independent irradiance observations that have a physically based degradation correction [*Harder et al.*, 2009, auxiliary material]. We present a modeling study on the impact of SORCE SSI variability on middle atmospheric ozone.

[3] Up to the present time, most climate and solar cycle related modeling studies have relied on solar input spectra that are scaled by long-term proxies of solar activity such as the F10.7 radio flux [*Marsh et al.*, 2007; *Randel and Wu*, 1999] or an equivalent Mg II core-to-wing [*Soukharev and Hood*, 2006]. A more dependable solar model employs solar irradiance reconstructions based on combined sunspot and facular proxy indicators (predominately the photometric sunspot index and the Mg II index) such as the Naval Research Laboratory SSI model (NRLSSI) [*Lean*, 2000]. The NRLSSI model has recently been employed as solar input for climate model inter-comparison studies [*Eyring et al.*, 2010; *Morgenstern et al.*, 2010]. However, solar observations from the SORCE instruments shows that there is more spectral variability over the declining phase of solar cycle 23 than previously estimated. The SORCE data show that the SSI values for wavelengths with brightness temperatures greater than 5770 K brighten with decreasing solar activity, whereas those with lower brightness temperatures show a dimming. These results indicate that different parts of the solar atmosphere contribute differently to the TSI with the behavior in the deep photospheric layers giving an opposing and nearly compensating trend in the upper layers of the sun. These observed effects are not captured in semi-empirical SSI models [*Harder et al.*, 2009]. We investigate the impact of enhanced spectral variability on middle atmospheric ozone with simulations using WACCM, a comprehensive chemical climate model. Simulations that use a proxy-based solar model are compared and contrasted to a simulation that uses solar irradiance observations compiled from SOLSTICE (110–240 nm) and SIM (240–2400 nm) [*McClintock et al.*, 2005; *Harder et al.*, 2010, and references therein]. This study applies a state-of-the-art global circulation model (GCM) with interactive chemistry to investigate more thoroughly the responses found by *Haigh et al.* [2010]. In addition, we present observational analyses of ozone measurements reported by the TIMED-SABER instrument. The observed ozone variations in the lower mesosphere have major features in

[1] Laboratory for Atmospheric and Space Physics, University of Colorado at Boulder, Boulder, Colorado, USA.
[2] Atmospheric Chemistry Division, National Center for Atmospheric Research, Boulder, Colorado, USA.

0094-8276/11/2011GL047561

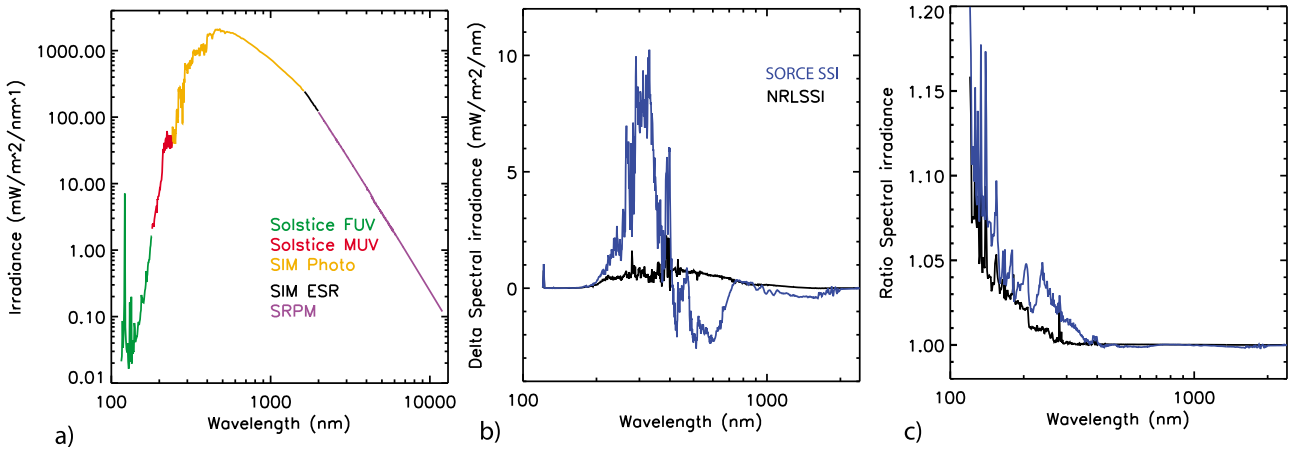

Figure 1. (a) Composite solar spectra of 2004. SORCE SOLSTICE from 116–240 nm, SORCE SIM from 240 nm to 2 μm, and the Solar Radiation Physical Modeling (SRPM) from 2 to 11 μm. (b) Spectral difference 2004–2007. (c) Spectral ratio 2004/2007.

common with the predictions from the WACCM simulations that use SORCE SSI input.

2. Model Simulations

[4] WACCM 3.5 is a fully coupled chemistry, radiation and dynamics global model extending from the surface to the thermosphere based on version 3 of the Community Atmosphere Model (CAM3) [*Garcia et al.*, 2007, 2011]. WACCM was validated under the CCMVal project of SPARC (Stratospheric Processes and their Role in Climate [*Eyring et al.*, 2010; *Morgenstern et al.*, 2010]) and shown to produce realistic ozone trends.

[5] Because the SPARC 2010 CCMVal project [*Eyring et al.*, 2010] recommends the use of the NRLSSI model as solar input for climate studies, we perform three WACCM experiments with fixed solar forcing based on NRLSSI and SORCE SSI. Each experiment was initialized from NCAR's CCMVal SPARC simulations and year 2004 of this simulation was perpetually run in all three cases with fixed greenhouse gases. This was done to ensure that the dominant source of atmospheric variability was the response from the solar forcing. Each experiment was integrated for 24 years. Experiment 1 used the NRLSSI spectra averaged over Aug. 8–Oct. 19, 2007 to represent quiet Sun conditions. Experiment 2 used NRLSS spectra averaged over Oct. 1–24, 2004, to represent high solar activity but is free from the short-lived contributions due to the passage sunspots and their associated plage regions. Experiment 3 is constructed from the SORCE SSI composite spectrum shown in Figure 1a. Figure 1b shows the irradiance differences for both SORCE and NRLSSI for the same 2004 and 2007 time periods. Because differences in the absolute calibration between SORCE and NRL spectra can generate spurious atmospheric signals that would complicate the interpretation of the model results [*Zhong et al.*, 2008], we use the NRLSSI 2007 quiet spectrum and scale it to represent the high activity case observed in the 2004 SORCE data. Figure 1c shows the ratio of the SORCE 2004 to 2007 spectra; this ratio is multiplied by the low activity NRLSSI 2007 spectrum to give the input spectrum for Experiment 3. Thus the Experiment 3 input spectrum has the SORCE SSI variability imposed on the NRLSSI irradiance calibration. It must be emphasized that the TSI is the same for the Experiments 1 and 3 input spectra, but the spectral distribution is distinctly different (Figures 1b and 1c). A detailed description of the SORCE solar input is presented in the auxiliary material.[1]

[6] The yearly perpetual simulations are averaged to produce a representative average year per case. This is to reduce the random component of a free running model and to identify the significance of the results. Figures 2a, 2b, 2e, and 2f present the latitude-height maps of the percent difference (active – quiet) of the ozone annual average for both the SORCE and NRLSSI case study simulations. The unshaded regions are significant to 95%. Due to the diurnal cycle and local time solar response of ozone [*Marsh et al.*, 2003], the results are separated into day and night. The percent difference for the SORCE case study (Figures 2b and 2f) produce an altitude structure very different than the NRLSSI case study results (Figures 2a and 2e). The daytime NRLSSI spectral solar input produces an ozone altitude structure that shows a higher concentration at solar active (2004) conditions than at solar quiet (2007) conditions with a maximum difference of 1% around 40 km (Figure 2a). The daytime ozone response to SORCE input spectra produces an atmospheric structure that is similar at low altitudes but is distinctly different above 40 km. There is a clear sign change in the ozone response that is not present in the NRLSSI study above 40 km, indicating an increase in ozone from 2004 to 2007 in the mesosphere. More UV variability causes the lower mesospheric ozone to respond out-of-phase to the solar cycle trend, whereas the stratosphere responds in-phase. Both the NRLSSI (Figure 2e) and SORCE (Figure 2f) nighttime conditions show a different mesospheric response in the absence of photolysis.

3. Comparison to SABER Observations

[7] With such distinct differences in the ozone response of the two solar scenarios modeled with WACCM, it is pertinent to look for the signal in observations. There are two

[1] Auxiliary materials are available in the HTML. doi:10.1029/2011GL047561

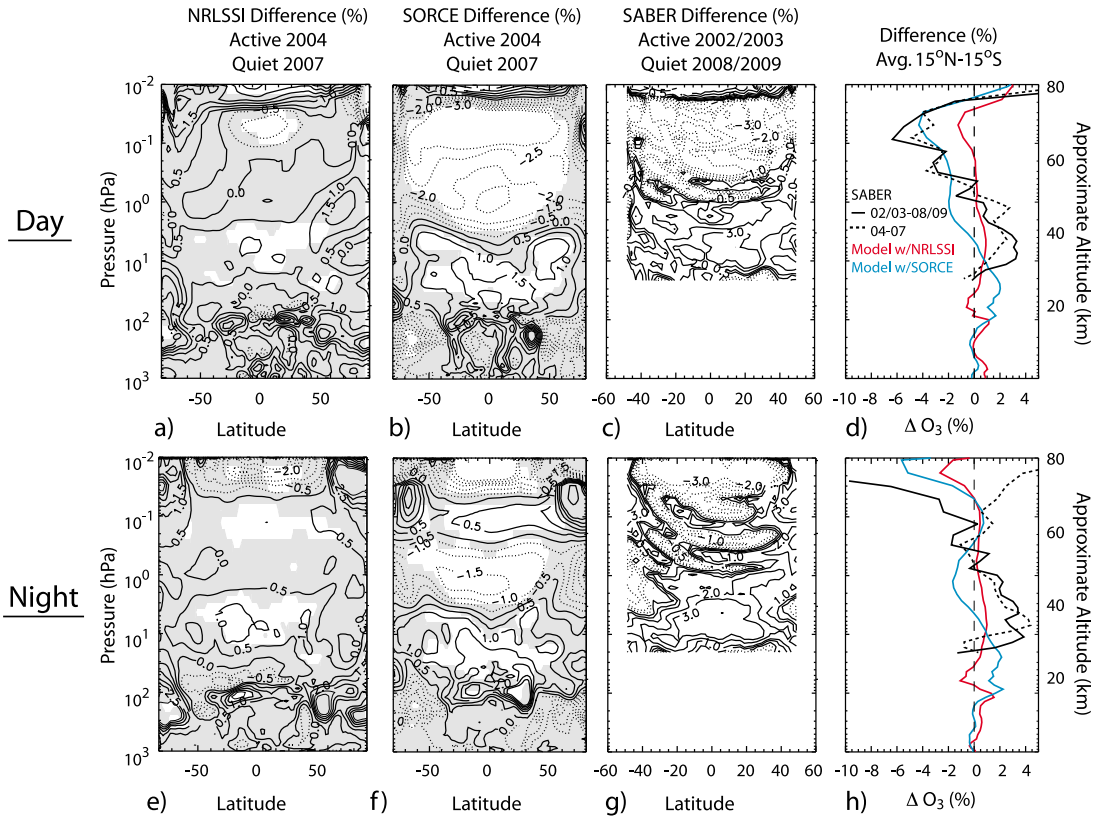

Figure 2. Annual mean ozone percent difference (max-min). (a and e) The day and night WACCM ozone percent difference (2004–2007) forced with NRLSSI. (b and f) The day and night WACCM ozone percent difference (2004–2007) forced with SORCE SSI. The unshaded regions are at the 95% confidence level. (c and g) The day and night SABER ozone percent difference (2002/2003–2008/2009). (d and h) The equatorial day and night altitude profiles of percent difference derived from Figures 2a, 2b, 2c, 2e, 2f, and 2g.

available ozone datasets that comply with the observational requirements needed to identify the mesospheric signal (i.e., that cover the time period in question, include consistent global and local time sampling, and altitude profiles up through the mesosphere): the Microwave Limb Sounder (MLS) and SABER. *Haigh et al.* [2010] showed a distinct ozone phase change above 40 km in MLS ozone measurements. To expand on that research we present the results from SABER.

[8] The O_3 emission measurements from the 9.6 μm channel on TIMED-SABER are used for this analysis [*Rong et al.*, 2009]. The data span 9 years (2002–2010) and provide very good sampling (good global and local time coverage). The data are separated into day and night average time sequences (monthly and annually). The first 6 months of SABER data are not used to eliminate possible biases due to the reported ice buildup on the detector. The O_3 mixing ratio data are screened to eliminate outliers by omitting the profiles with the top 1% of mixing ratios at each pressure. We present annual average differences to compare to the model results shown in Figure 2.

[9] Figures 2c and 2g show the percent difference between the SABER O_3 annual mean of solar maximum (2002/2003) and solar minimum (2008/2009) conditions, taking advantage of the SABER time coverage. The contour plot of the 2004–2007 SABER O_3 percent difference (for direct comparison to the model results) is not shown because the altitude structure is very similar to Figures 2c and 2g. In general, SABER O_3 latitude/altitude structure is more similar to the WACCM model results with SORCE SSI input than to model results with NRLSSI input. The most noticeable similarity is that SABER data shows a clear sign change in mesospheric ozone. The comparisons imply that higher UV variability can improve the model/data comparison of daytime mesospheric ozone. The sign change between positive in the stratosphere and negative in the mesosphere is less apparent in the night data, with the differences oscillating around zero from 1 hPa to 0.1 hPa (Figure 2g). By separating into day and night, the SABER data suggests that photochemical processes could be a major source of producing the out-of-phase relationship of ozone with solar cycle in the lower mesosphere.

[10] Figures 2d and 2h show average equatorial altitude profiles from the accompanying contour plots. In the daytime mesosphere, the SORCE simulation shows greater similarity with the SABER data than the NRLSSI simulation. Included in Figures 2d and 2h is the SABER annual difference from 2004 to 2007 for direct comparison to the model simulations for the same years. The 2004–2007 percent difference near 0.1 hPa is in even better agreement with the SORCE model estimate. However, the ozone structure in the stratosphere does not agree between data and model. Referencing the contour maps, it is evident that the sign change in the SORCE model simulation occurs near

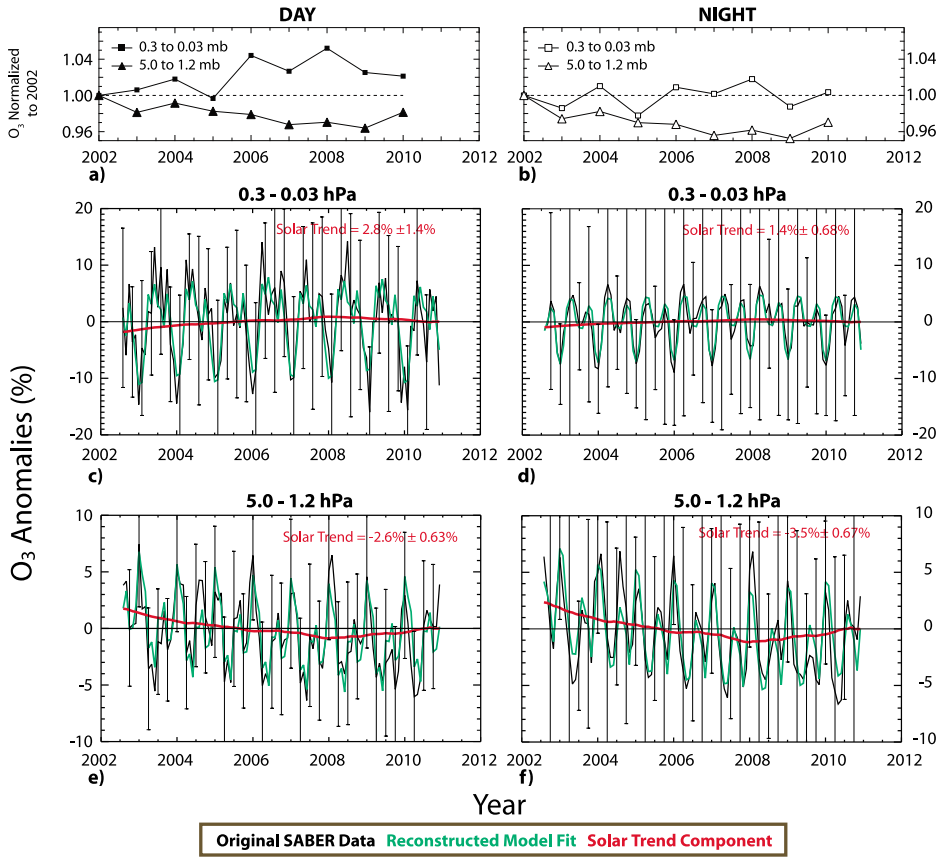

Figure 3. (a and b) The day and night SABER ozone annual mean time series normalized to 2002. Figures 3a and 3b show time series averaged over the pressure ranges 0.3 hPa and 0.03 hPa and 5 hPa and 1.2 hPa. (c–f) Day and night monthly mean SABER ozone concentrations. The data (solid black lines) are percentage anomalies of tropical (15°S–15°N) monthly means from July 2002 to December 2010. The values reconstructed from a 3-component regression model are shown as green lines. The solar component of the regression 16 is shown in red. Figures 3c and 3d are averaged between 0.3 hPa and 0.03 hPa. Figures 3e and 3f are averaged between 5 hPa and 1.2 hPa.

5 hPa, while the SABER results show a transition near 1 hPa. While the SORCE model simulation gives a better representation of the SABER results than the NRLSSI study, it is apparent that the SORCE WACCM simulation needs further refinements. One possibility for the 10 km differential in the location of the sign change between model and SABER could be attributed to the uncertainty in the measured SORCE irradiance values between 200–400 nm as demonstrated by *Haigh et al.* [2010]. Future work is planned to further quantify errors in SORCE SSI and characterize the impact in GCM simulations.

[11] Figures 3a and 3b show the annual mean equatorial time series of the day and nighttime SABER data averaged over two pressure ranges corresponding to the lower mesosphere (0.3–0.03 hPa) and the stratosphere (5–1.2 hPa) regions of the atmosphere. Each time series is normalized to the first year to highlight the variations. The daytime mesosphere shows an increase in ozone of 3.8%, while the stratospheric time series show a decrease in ozone of 4% over the 2002 to 2009 time span. The daytime and nighttime stratospheric curves are very similar since ozone has very little diurnal variation there. The night and day variations in the mesosphere are quite different. In the lower mesosphere, the primary loss of odd oxygen (O_x = O_3+O) is due to reactions with the hydrogen family (HO_x). Both this loss and the production of odd oxygen from O_2 photolysis cease at night. The daytime response is apparent in every available SABER year, and the annual trends are reversing as the sun comes out of solar minimum starting in 2009.

[12] Figures 3c–3f show a multiple linear regression of the SABER ozone monthly averaged day and nighttime series. The SABER data are presented as percent anomalies of tropical monthly means from July 2002 through December 2010 averaged over the presented pressure ranges. To be consistent with *Haigh et al.* [2010] we used the identical regression code (Myles Allen, Oxford University, see auxiliary material for code). The regression analysis was carried out on the deseasonalized time series with three regression indices: two quasi-biennial oscillation (QBO) components (from 30 hPa) out of phase by $^1/_4$ wavelength [*Matthes et al.*, 2004], and a solar component. The usable SIM observations start in 2004 and therefore cannot directly be used to construct a solar component for the regression. Therefore to extend the SIM UV variability back to 2002, prior to the launch of the SORCE mission, we use images from the Precision Solar Photometric Telescope (PSPT) at the Rome Observatory [*Criscouli et al.*, 2008] to estimate the time evolution of solar activity over this time period. The active network corresponds to the slowly decaying bright-

ness contribution in the PSPT Ca II solar images [*Fontenla and Harder*, 2005].

[13] The results are consistent with Figures 3a and 3b and are significant to the 95% level. The daytime lower mesosphere (Figure 3c) shows a 2.8% increase in ozone along the declining phase of solar cycle 23. The stratosphere shows the opposite response and is in phase with the solar cycle with a 2.6% reduction in ozone (Figure 3e). The lower mesosphere nighttime signal is flat, illustrating a reduced magnitude of the response, although there is a small 1.4% increasing trend (Figure 3d). The nighttime stratosphere is very similar to the daytime with a decreasing trend of 3.5% (Figure 3f). Figure 3 also indicates that the variations respond to the upswing of the solar cycle in the middle of 2009, suggesting that the signal is solar cycle induced. These results are congruent with the 2004–2008 MLS analysis by *Haigh et al.* [2010] where mesospheric ozone (0.68–0.32 hPa) increased by 1.7% and stratospheric ozone decreased by 4.5% (10.0–6.8 hPa).

4. Discussion

[14] A number of previous model studies have shown that, over part of the lower to middle mesosphere, ozone decreases with increasing solar flux. This is understood to be due to increases in the rate of water photolysis, which leads to faster ozone destruction by HO_x catalytic cycles. We have shown here that the lower mesospheric ozone decrease in response to the solar cycle may have substantially larger magnitude and cover a more extensive altitude range than previously simulated. Model simulations and satellite observations support this conclusion. The difference in the model results is due to an increase in UV variability as measured by the SORCE mission. Although the simulations have some differences with the observations, overall the agreement supports the new solar SSI data.

[15] The SABER tropical stratospheric ozone response to solar cycle is consistent with results presented by *Remsberg* [2008] (Halogen Occultation Experiment, HALOE) and *Soukharev and Hood* [2006] (Solar Backscatter Ultraviolet, SBUV). Like HALOE and SBUV, the SABER max – min response peaks near 5 hPa with a 2–3% amplitude (Figure 2d). In addition, all three datasets indicate that the solar ozone response decreases to 0% around 1 hPa. While the HALOE and SBUV analyses stop at 1 hPa, SABER is able to resolve the mesospheric response and demonstrates that the ozone trend is negative above 1 hPa. It is important to note that this result would not be detected in the total ozone response to solar cycle [*Hood*, 1997] since the mesospheric signal contributes only 1% to the total.

[16] *Marsh et al.* [2007] demonstrated that lower mesosphere ozone is sensitive to the photochemistry of HO_x. In addition, *Dikty et al.* [2010] showed that daytime ozone is driven by photochemistry and less influenced by transport. This dependence is clearly evident in the presented day/night results. In the lower mesosphere, the primary loss of odd oxygen is due to HO_x reactions. More UV at solar active conditions leads to an enhancement of O_3 photolysis. This leads to more $O(^1D)$ and therefore more OH through the reaction of $O(^1D)$ with H_2O. Ozone is depleted through several catalytic processes with OH and H [*Grenfell et al.*, 2006]. More UV is also transmitted to the stratosphere leading to greater O_2 photolysis and therefore more stratospheric O_3.

[17] Based on these findings, this work extends and confirms *Haigh et al.*'s [2010] study in the following ways: a) utilizes a 3-d GCM with chemistry rather than a static 2-d stratospheric model; b) uses 9 years of SABER ozone data that covers the full descending phase of solar cycle 23 in place of the 4-year MLS record; c) detects the out-of-phase ozone response in an independent instrument observation with similar linear trends; d) segregates by day and night to isolate photochemical effects. This work alleviates some of the concerns voiced by *Garcia* [2010] by conducting an independent analysis on a longer data record. Continued and concurrent measurements of solar SSI and mesospheric ozone are needed to corroborate the conclusions of this study.

[18] **Acknowledgments.** We wish to thank Martin Snow (LASP) and Ilaria Ermolli (Rome Observatory) for providing data used in this study. The WACCM simulations were conducted at the NASA Ames Advanced Computing Division, Ames Research Center, CA. This research was supported by NASA contract NAS5-97045. A. Smith and D. Marsh are supported by the National Center for Atmospheric Research and the National Science Foundation.

[19] The Editor thanks two anonymous reviewers for their assistance in evaluating this paper.

References

Criscouli, S., et al. (2008), Radiative emission of solar features in Ca II K, *Mem. Soc. Astron. Ital.*, *81*, 773.

Dikty, S., et al. (2010), Daytime ozone and temperature variations in the mesosphere: A comparison between SABER observations and HAMMONIA model, *Atmos. Chem. Phys.*, *10*, 8331–8339, doi:10.5194/acp-10-8331-2010.

Eyring, V., et al. (2010), Stratospheric Processes and Their Role in Climate (SPARC) report on the evaluation of chemistry-climate models, *SPARC Rep. 4*, World Meteorol. Organ, Geneva, Switzerland.

Fontenla, J. M., and J. Harder (2005), Physical modeling of spectral irradiance variations, *Mem. Soc. Astron. Ital.*, *76*, 826.

Garcia, R. R. (2010), A solar surprise?, *Nature*, *467*, 668–669, doi:10.1038/467668a.

Garcia, R. R., D. R. Marsh, D. E. Kinnison, B. A. Boville, and F. Sassi (2007), Simulation of secular trends in the middle atmosphere, 1950–2003, *J. Geophys. Res.*, *112*, D09301, doi:10.1029/2006JD007485.

Garcia, R. R., et al. (2011), On the determination of age of air trends from atmospheric trace species, *J. Atmos. Sci.*, *68*, 139–154, doi:10.1175/2010JAS3527.1.

Grenfell, J. L., R. Lehmann, P. Mieth, U. Langematz, and B. Steil (2006), Chemical reaction pathway affecting stratospheric and mesospheric ozone, *J. Geophys. Res.*, *111*, D17311, doi:10.1029/2004JD005713.

Haigh, J. D., et al. (2010), An influence of solar spectral variations on radiative forcing of climate, *Nature*, *467*, 696–699, doi:10.1038/nature09426.

Harder, J. W., J. M. Fontenla, P. Pilewskie, E. C. Richard, and T. N. Woods (2009), Trends in solar spectral irradiance variability in the visible and infrared, *Geophys. Res. Lett.*, *36*, L07801, doi:10.1029/2008GL036797.

Harder, J. W., et al. (2010), The SORCE SIM solar Spectrum: Comparison with recent observations, *Sol. Phys.*, *263*, 3–24, doi:10.1007/s11207-010-9555-y.

Hood, L. (1997), The solar cycle variation of total ozone: Dynamical forcing in the lower stratosphere, *J. Geophys. Res.*, *102*, 1355–1370, doi:10.1029/96JD00210.

Lean, J. (2000), Evolution of the Sun's spectral irradiance since the Maunder Minimum, *Geophys. Res. Lett.*, *27*, 2425–2428, doi:10.1029/2000GL000043.

Marsh, D., A. Smith, and E. Noble (2003), Mesospheric ozone response to changes in water vapor, *J. Geophys. Res.*, *108*(D3), 4109, doi:10.1029/2002JD002705.

Marsh, D. R., R. R. Garcia, D. E. Kinnison, B. A. Boville, F. Sassi, S. C. Solomon, and K. Matthes (2007), Modeling the whole atmosphere response to solar cycle changes in radiative and geomagnetic forcing, *J. Geophys. Res.*, *112*, D23306, doi:10.1029/2006JD008306.

Matthes, K., U. Langematz, L. L. Gray, K. Kodera, and K. Labitzke (2004), Improved 11-year solar signal in the Freie Universität Berlin Climate

Middle Atmosphere Model (FUB-CMAM), *J. Geophys. Res.*, *109*, D06101, doi:10.1029/2003JD004012.

McClintock, W. E., et al. (2005), Solar-Stellar Irradiance Comparison Experiment II (SOLSTICE II): Instrument concept and design, *Sol. Phys.*, *230*, 225–258, doi:10.1007/s11207-005-7432-x.

Morgenstern, O., et al. (2010), Review of the formulation of present-generation stratospheric chemistry-climate models and associated external forcings, *J. Geophys. Res.*, *115*, D00M02, doi:10.1029/2009JD013728.

Randel, W. J., and F. Wu (1999), A stratospheric ozone trends data set for global modeling studies, *Geophys. Res. Lett.*, *26*(20), 3089–3092, doi:10.1029/1999GL900615.

Remsberg, E. E. (2008), On the response of Halogen Occultation Experiment (HALOE) stratospheric ozone and temperature to the 11-year solar cycle forcing, *J. Geophys. Res.*, *113*, D22304. doi:10.1029/2008JD010189

Rong, P. P., J. M. Russell III, M. G. Mlynczak, E. E. Remsberg, B. T. Marshall, L. L. Gordley, and M. López-Puertas (2009), Validation of TIMED/SABER v1.07 ozone at 9.6 μm in the altitude range 15–70 km, *J. Geophys. Res.*, *114*, D04306, doi:10.1029/2008JD010073.

Soukharev, B. E., and L. L. Hood (2006), The solar cycle variation of stratospheric ozone: Multiple regression analysis of long-term satellite data sets and comparisons with models, *J. Geophys. Res.*, *111*, D20314, doi:10.1029/2006JD007107.

Zhong, W., S. M. Osprey, L. J. Gray, and J. D. Haigh (2008), Influence of the prescribed solar spectrum on calculations of atmospheric temperature, *Geophys. Res. Lett.*, *35*, L22813, doi:10.1029/2008GL035993.

J. M. Fontenla, J. W. Harder, A. W. Merkel, and T. N. Woods, Laboratory for Atmospheric and Space Physics, University of Colorado at Boulder, 1234 Innovation Dr., Boulder, CO 80303, USA. (aimee.merkel@colorado.edu)

D. R. Marsh and A. K. Smith, Atmospheric Chemistry Division, National Center for Atmospheric Research, PO Box 3000, Boulder, CO 80307, USA.